Electronic Journal of Structural Engineering

Original Article

Cite this: DOI:10.56748/ejse.24878

Received Date: 8 September 2025
Accepted Date:10 November 2025

1443-9255
https://ejsei.com/ejse

Strain Hardening Behavior of Engineered Cementitious / Geopolymer Composites Under Sulfuric Acid Erosion

Ghassan Hussein Humur [a], Haider Turki Abed [b], Alaa Mohammedameen [c], Diyar N. Qader [a*]

[a] Department of Civil Engineering, University of Kirkuk, Kirkuk, Iraq
[b] Department of Civil Engineering, University of Tikrit, Saladin, Iraq
[c] Construction Engineering and Project Management Department, Akre University for Applied Science, Duhok, Iraq
*Corresponding author: diyar.nasih@uokirkuk.edu.iq

Abstract

This study presents a comparative durability assessment of lightweight Engineered Geopolymer Composites (EGCs) against a lightweight Engineered Cementitious Composite (ECC) under prolonged sulfuric acid (H_2SO_4) attack. This work addresses a critical gap by systematically comparing the strain-hardening performance and degradation mechanisms of lightweight fiber-reinforced composites under aggressive chemical exposure. Four lightweight mixtures, three EGCs with varying slag/fly ash contents (S-EGC: 100% slag; FAS-EGC: 50% slag; FA-EGC: 100% fly ash) and one lightweight ECC control, were fabricated using expanded glass granule (EGG) aggregates and immersed in a 5% H_2SO_4 solution for up to 120 days. Before exposure, the incorporation of slag significantly enhanced pre-exposure mechanical properties; S-EGC showed the highest ultimate strength, while the FAS-EGC mixture provided the best balance of strength and ductility, achieving a tensile strain capacity of 3.21%. The lightweight EGCs demonstrated superior acid resistance compared to the lightweight ECC. After 120 days of exposure, the S-EGC composite retained the highest residual compressive strength (81.59%), while the ECC retained significantly less. Significantly, all exposed EGC and ECC specimens maintained their multiple cracking and deflection-hardening behavior, retaining approximately 50% of their total deflection capacity after four months. Microstructural analysis confirmed that the superior resistance of S-EGC is attributed to its stable, cross-linked alumino-silicate polymer structure. These findings confirm that lightweight slag-based EGCs are a highly durable and ductile sustainable alternative for structural applications in aggressive environmental settings, such as wastewater treatment infrastructure and chemical plants.

Keywords

Engineered geopolymer composites, Durability properties, Sulfuric acid, Tensile performance, Deflection-hardening behavior, Microstructural analysis

1. Introduction

The increasing severity of environmental conditions in urban and industrial infrastructure demands the development of construction materials with not only superior mechanical performance but also enhanced durability (Li 2008). Among the most aggressive environments, exposure to sulfuric acid (H2SO4) in wastewater systems, chemical processing facilities, and drainage networks remains a primary cause of concrete degradation, resulting in high maintenance costs and reduced service life (Li 2019; Shumuye et al. 2023). To overcome the inherent brittleness and durability limitations of conventional concrete, Engineered Cementitious Composites (ECCs) were micromechanically designed to exhibit exceptional damage tolerance and ductility (Li 2008). ECC is characterized by low volume fractions (typically <2%) of short, randomly distributed polymeric fibers within a Portland cement-based mortar (Niş, Eren, and Çevik 2023; Y. Zhang and Chen 2023). This specialized matrix design enables strain-hardening behavior, allowing the material to reach tensile strains of ~3-5% through the formation of multiple, extremely fine microcracks, thereby greatly increasing the lifespan and resilience of civil infrastructure (Mustafa et al. 2009; Niş et al. 2024; Q. Yang et al. 2025). Despite their remarkable performance, standard ECC mixtures typically contain two to three times the amount of Ordinary Portland Cement (OPC) compared to normal concrete, resulting in a significant carbon and energy footprint (Abed et al. 2022; Hu 2023; Malhotra 1999; Thampy, Dadi, and Sharma 2024). Given that OPC production accounts for approximately 7% of global CO2 emissions, the construction industry is urgently seeking sustainable alternatives (Abed et al. 2022; Hu 2023; Malhotra 1999; Thampy, Dadi, and Sharma 2024).

Engineered Geopolymer Composites (EGCs) represent a highly promising and sustainable alternative to ECC and conventional concrete (Abdulhaleem et al. 2025; Abed et al. 2022; G. Humur and Çevik 2022a; Qader et al. 2025). Using industrial waste materials such as fly ash and ground granulated blast furnace slag (GGBS) as cement-free precursors, EGCs inherently possess a lower carbon footprint and offer superior environmental sustainability (Lao et al. 2024; Nematollahi, Sanjayan, and Shaikh 2016; Ohno and Li 2018). Comparative life-cycle assessments have demonstrated that conventional EGC mixtures emit up to 52% less carbon dioxide and have a more than 17% lower embodied energy than typical ECC mixtures, mainly due to the substitution of OPC with by-product materials (Nematollahi et al. 2017). Like their cementitious counterparts, EGCs are fiber-reinforced and exhibit high tensile ductility, strain-hardening, and tight crack width control due to strong adhesion between the fiber and the geopolymer matrix (Ghassan Hussein Humur and Çevik 2024; Ohno and Li 2014; Revathy, Yaswanth, and Gajalakshmi 2023). The mechanical properties of EGCs are significantly influenced by their binder composition. Numerous studies have investigated how precursor ratios, specifically the inclusion of slag, affect the composite performance (Abdulhaleem et al. 2025; Revathy, Yaswanth, and Gajalakshmi 2023). Generally, an increase in slag concentration leads to enhanced properties, including higher compressive strength, flexural strength, and ultimate tensile stress (Ghassan H Humur et al. 2025; Lao et al. 2023; Ling et al. 2019). Conversely, optimizing parameters like the activator concentration, fiber type, and sand concentration is critical to sustain the desirable pseudo-strain hardening behavior and avoid increases in matrix fracture toughness that could lead to brittle failure (Güneş, Öz, and Yücel 2024; Nematollahi, Sanjayan, and Shaikh 2016; Zahid et al. 2020).

The chemical resistance of geopolymer materials is often cited as superior to OPC-based binders due to the stable, highly polymerized alumino-silicate structure formed during alkali activation (Sá Ribeiro et al. 2021). Studies on geopolymer concrete have reported enhanced durability under H2SO4 exposure compared to conventional concrete (R. Alzeebaree et al. 2019; Kurtoglu, A.E., Alzeebaree, R., Aljumaili, O., Nis, A., Gulsan, M.E., Humur, G. and Cevik, A 2018). For ECC, research has also shown that specialized additives, such as graphene oxide, can improve acid resistance (Sabapathy et al. 2020), though exposure to simulated acidic conditions has still resulted in noticeable reductions in tensile strength and ductility (Wu et al. 2020). Critically, only limited studies have directly compared EGC and ECC durability. Ohno et al. (Ohno and Li 2019) reported that fly-ash-based EGC showed negligible mechanical degradation under acid attack, with a mass loss rate three times lower than that of conventional concrete and superior performance to ECC. A simultaneous area of development involves lightweighting the composite through the use of low-density aggregates, such as Expanded Glass Granule (EGG) aggregates, to reduce structural dead load (Mustafa et al. 2009; Z. Zhang et al. 2023). However, this modification introduces new variables, as both the lightweight aggregate and the lightweight matrix composition may alter the chemical resistance and mechanical response under prolonged acid

attack. To the best of the authors' knowledge, a critical research gap exists: there is a distinct lack of systematic, long-term comparative analysis focusing on the acid resistance of lightweight EGCs (with varying slag/fly ash contents) and lightweight ECCs that utilize EGG aggregates. More importantly, the ability of these lightweight, high-performance composites to retain their characteristic strain-hardening and deflection capacity after prolonged chemical exposure has not been rigorously studied or quantified.

This study addresses this gap by presenting a novel, comprehensive, and comparative durability assessment of lightweight Engineered Geopolymer Composites (EGCs), formulated with different slag and fly ash ratios, against a lightweight Engineered Cementitious Composite (ECC). All mixtures were subjected to prolonged H2SO4 acid attack for 120 days. The primary contribution of this work lies in the integrated analysis of residual mechanical properties (compressive, flexural, and, crucially, tensile strain-hardening) and microstructural degradation (SEM/EDX) after acid exposure. The aim is to rigorously evaluate the effect of precursor chemistry on long-term durability and identify the optimal, most resilient, and sustainable lightweight composite suitable for structural application in severely acidic environmental settings.

2. Materials and test techniques

2.1 Materials and mixed characteristics

This study utilized a distinct set of materials for manufacturing the lightweight Engineered Geopolymer Composites (EGCs) and the lightweight Engineered Cementitious Composite (ECC) control mixture. The ECC was produced using Ordinary Portland Cement (OPC) and Class F Fly Ash (FA), while the EGCs were fabricated using a combination of Class F FA and Ground Granulated Blast Furnace Slag (GGBFS) as the main pozzolanic bonding materials. The chemical compositions of the GGBFS, FA, and OPC, determined via X-ray Fluorescence (XRF) analysis, are provided in Table 1. All mixtures incorporated lightweight aggregates to achieve low density. Expanded Glass Granule (EGG) aggregate, a recycled glass product, was used in combination with silica sand. The EGG granules, sourced from PerHAbbe in Kocaeli, Turkey, are white to creamy in color, sized between 0.1 and 0.25 mm, possess a low bulk density of 450 kg/m3, and exhibit a crushing resistance of 3.1 N/cm2. The chemical composition of the recycled glass EGG is detailed in Table 2. Polyvinyl Alcohol (PVA) fibers were used as the primary reinforcement for all composites to ensure high ductility and strain-hardening behavior. The key properties of the PVA fiber, including length and diameter, are provided in Table 3. Crucially, the fiber surface was coated with a proprietary hydrophobic oiling agent at 1.2% by mass to tailor the interfacial properties between the fiber and the matrix, a requirement for achieving micromechanically stable multiple-cracking performance in both ECC and EGC (E.-H. Yang et al. 2009). A constant fiber volume fraction of 2% was maintained across all mixtures. For the EGC mixtures, an alkaline solution comprising Sodium Hydroxide (NaOH) pellets and Water Glass (Na2SiO3) was used to activate the pozzolanic precursors. Sodium Hydroxide: Pellets of 97-98% purity were dissolved in tap water to create a 12M molar concentration solution 24 hours prior to mixing. The selection of 12M NaOH molarity was based on literature recommendations for optimizing geopolymerization efficiency, mechanical strength, and long-term durability (R. Alzeebaree et al. 2019; Kurtoglu, A.E., Alzeebaree, R., Aljumaili, O., Nis, A., Gulsan, M.E., Humur, G. and Cevik, A 2018). Water Glass obtained from Istanbul, Turkey, the commercial solution had a density of 1373 kg/m3 and contained 27.33% SiO2 and 8.81% Na2O. A fixed mass ratio of Na2SiO3/NaOH = 2.5 was chosen for the alkaline activator solution, as previous studies demonstrated this ratio achieves optimal rheological, mechanical, and ductility characteristics in EGC (Hardjito et al. 2004; Sahmaran, Li, and Li 2007; Temuujin, van Riessen, and MacKenzie 2010). In addition, a Polycarboxylate-High Range Water Reducing Admixture (PHRWRA) was utilized in the EGC mixtures (Wu et al. 2020). An extra quantity of water (20 kg/m3) was intentionally added to the geopolymer mixtures. Unlike OPC hydration, the role of this added water in alkali-activated materials is not primarily for a chemical reaction but for optimizing workability, controlling reaction kinetics, and facilitating microstructural development (Gülşan et al. 2018; Sahmaran, Li, and Li 2007). The study evaluated four distinct lightweight mixtures, with all mix quantities presented in Table 4. EGC Mixes: All EGC mixtures maintained a constant mass ratio of pozzolanic materials (FA + Slag) to alkaline liquid of 0.45. The ratio of EGG to pozzolanic materials was fixed at 0.20, which was optimized in prior research to achieve a balance of mechanical, ductility, and rheological performance (Aljanabi et al. 2022; G. Humur and Çevik 2022a). Three different EGC precursor ratios were prepared for comparative analysis: FA-EGC: 100% Fly Ash, 0% Slag. FAS-EGC: 50% Fly Ash, 50% Slag. S-EGC: 0% Fly Ash, 100% Slag.ECC Mix: The lightweight ECC mixture was designed with a constant water-to-cementitious material ratio of 0.29 and a fixed mass ratio of fly ash to cement of 0.5. Figure 1 illustrates the materials used in the production of ECC and EGC mixtures.

Fig.1 Source materials used in the production of ECC and EGC mixtures

Table 1. XRF and chemical composition of GGBFS, FA, and OPC.

Type	OPC	GGBFS	FA
SiO_2	19.69	36.4	62.53
Al_2O_3	5.16	10.39	21.14
CaO	62.12	34.12	1.57
Fe_2O_3	2.88	0.69	7.85
MgO	1.17	10.3	1.76
SO_3	2.63	0.49	0.10
K_2O	0.88	0.97	0.73
Na_2O	0.17	0.35	2.45
Loss of ignition	2.99	1.64	2.07
Blaine fineness (m^2/kg)	394	418	227
Specific gravity (kg/m^3)	3.15	2.79	2.04

Table 2. XRF analysis for expanded glass granule aggregate (EGG)

Chemical analysis	%
SiO_2	72.95
Na_2O	18.74
CaO	4.35
MgO	0.89
Al_2O_3	0.41
K_2O	0.2
TiO_2	0.03
FE_2O_3	0.09
Loss on Ignition	2.33

Table 3. Properties of PVA fibres

Fiber type	Tensile Strength (MPa)	Modulus of Elasticity (GPa)	Elongation (%)	Diameter (μm)	Length Density (mm) (g/cm)
PVA	1620	42.8	6	39	(8) (1.3)

Table 4. Mix ratios for EGC and ECC mixtures

Mix ID	Fly ash (kg/m^3)	Slag (kg/m^3)	Portland cement (kg/m^3)	Sodium hydroxide (kg/m^3)	Sodium silicate (kg/m^3)	Expanded glass granule (kg/m^3)	PVA (kg/m^3)	Superplasticizer (kg/m^3)	Additional water (kg/m^3)
FA-EGC	1000	0.0	0.0	128.57	321.43	200	26	20	20
FAS-EGC	500	500	0.0	128.57	321.43	200	26	40	20
S-EGC	0.0	1000	0.0	128.57	321.43	200	26	50	20
ECC	500	0.0	500.0	0.0	0.0	200	26	20	20

2.2 Mixing and curing

The preparation of the EGC and ECC specimens involved distinct mixing sequences and curing methods due to the fundamental differences in their binding chemistries (alkali-activation vs. hydration). Mixing Procedure: 1. Alkaline Activator Preparation (for EGC); The NaOH pellets were precisely measured to achieve the target 12M molarity and dissolved in tap water. This exothermic reaction produced a highly heated solution, which was then allowed to cool and stabilize at room temperature for at least 24 hours prior to mixing to ensure chemical consistency (Nematollahi, Sanjayan, and Ahmed Shaikh 2015; Nematollahi, Sanjayan, and Shaikh 2015). 2. Composite Mixing; The mixing process followed a standard two-stage approach for both EGC and ECC, conducted in a pan mixer. Dry Mixing (6 minutes): The solid components precursors (FA, GGBFS, or OPC), EGG aggregates, and silica sand were dry mixed for six minutes to ensure homogenization. Wet Mixing (3 minutes); The liquid components (Na2SiO3 solution, NaOH solution, and any extra water (EXW) were added to the dry blend. The mixture was then wet-mixed for three minutes. A Polycarboxylate-High Range Water Reducing Admixture (PHRWRA) was introduced to achieve the required flowability and workability. Fiber Incorporation (6–11 minutes); Polyvinyl Alcohol (PVA) fibers were added gradually to the homogeneous mixture. The mixing continued for an additional six minutes until the fibers were fully and uniformly dispersed. Spread-flow tests (mini-slumps) were performed both before and after fiber in addition to monitoring and ensure adequate rheological performance and uniform fiber distribution. The total mixing time for each batch was between 15 and 20 minutes. Fresh mixing, the fresh lightweight EGC and ECC mixtures were cast into various molds and consolidated using a vibrating table for one minute. The subsequent curing regimens were tailored to promote the optimal reaction kinetics for each composite type; To ensure full geopolymerization, particularly for the fly ash-rich mixtures, which require heat (Nematollahi, Sanjayan, and Ahmed Shaikh 2015; Nematollahi, Sanjayan, and Shaikh 2015). The freshly cast EGC specimens were placed in an oven and subjected to a controlled heat curing regime at 70 °C for 24 hours. To prevent moisture loss during this critical setting period, the specimens were carefully wrapped. After oven curing, the samples were removed, allowed to cool in the laboratory, demolded, and then stored at room temperature (23 °C) for a total 28-day maturation period prior to testing. ECC Curing (Hydration): In contrast, the OPC-based ECC specimens rely on traditional hydration. These samples were demolded after 24 hours and subjected to standard water curing by being immersed in tap water for the entire 28-day maturation period.

2.3 Test procedures

The mechanical and durability characteristics of the Engineered Geopolymer Composites (EGC) and Engineered Cementitious Composites (ECC) were comprehensively evaluated through a series of tests, including compression, uniaxial tension, and four-point flexural bending. The compressive strength for all EGC and ECC mixtures was determined using cubic specimens with nominal dimensions of 70.6 mm*70.6 mm*70.6 mm. The testing protocol was strictly followed the recommendations set forth by the Indian standard (IS: 4031-1968) (Japan Society of Civil Engineers 2008). To ensure statistical reliability, three identical specimens were tested for each mixture type, and the resultant average values were used for analysis. For the direct uniaxial tensile characterization of the EGC and ECC materials, coupon samples measuring 330 mm*60 mm*13 mm were prepared. These dimensions were selected in accordance with the relevant Japanese standard (e.g., JSCE-G 552-2009) (Japan Society of Civil Engineers 2008). The geometry was specifically chosen to be large enough to represent the composite's overall behavior, including the vital processes of multiple crack formation and strain-hardening characteristics, while remaining compatible with standard testing equipment. The size is optimized to ensure consistent and reproducible measurements of key tensile properties, such as ultimate tensile strength and strain capacity (Japan Society of Civil Engineers 2008). The flexural performance, which assessed the load-displacement response of the EGC and ECC composites, was evaluated using prism samples with dimensions of 330 mm*60 mm*13 mm in a four-point bending configuration (Mustafa et al. 2009). An electronic universal material testing equipment, capable of displacement control and possessing a maximum capacity of 500 kN, was utilized for both the tensile and flexural tests. A displacement-controlled loading rate of 0.2 mm/min was selected. This rate is consistent with established best practices for characterizing strain-hardening cementitious composites, as widely recommended by standards like ASTM C1609 and frequently applied in EGC and ECC research (ACI Committee 544 n.d.; ASTM n.d.). The slow loading rate is essential for allowing precise monitoring of the composite's post-cracking behavior and the development of ductility. Testing was continued until the specimen exhibited failure, marked by a significant drop in load, or until a target deflection was achieved (typically between 3 mm and 5 mm), aligning with methodologies reported in prior investigations (Ohno and Li 2018; E.-H. Yang et al. 2009). Following the mechanical characterization, particularly of the lightweight EGC samples that had been subjected to severe exposure conditions (such as sulfuric acid), microstructural analysis was performed. A ZEISS Gemini SEM 300 scanning electron microscopy (SEM) was employed to study the microstructure. The primary goal of this investigation was to identify the microstructural mechanisms and degradation processes responsible for the observed disparities in mechanical strength and durability.

2.4 Acid exposure

The durability of both the Engineered Cementitious Composites (ECC) and Engineered Geopolymer Composites (EGC) was assessed by exposing the specimens to a sulfuric acid (H2SO4) solution for a total period of 120 days. After the initial 28-day curing period, the specimens designated for durability testing were immersed in a 5% H2SO4 solution. In parallel, control samples from the same mixtures were maintained under ambient laboratory conditions (23 °C) until the scheduled age of testing to serve as unexposed reference materials. Prior to acid exposure, both the ECC and EGC specimens were saturated by soaking them in water for 24 hours. Subsequently, they were allowed to dry at 23 °C for two hours to establish their initial mass (M0). To ensure a consistent and aggressive exposure environment, the pH of the 5% H2SO4 solution was monitored weekly. If any notable shift in acidity occurred, the solution was immediately replaced with a fresh 5% H2SO4 solution to maintain the required concentration and exposure severity. At bi-weekly intervals, the specimens were retrieved from the acid solution and rinsed thoroughly with water to remove any chemical residue or precipitated reaction products from the surface. Following a two-hour drying period at 23 °C, the specimens' mass was recorded. The extent of chemical deterioration due to the acid attack was primarily quantified by monitoring the weight change of the exposed samples at 30, 60, 90, and 120-day intervals. The relative change in mass was calculated using Equation (1) (Z. Zhang et al. 2020):

$$Mass\ loss(\%) = \frac{m_0 - m_1}{m_0} 100 \quad (1)$$

Where m_0 is the initial mass of the specimen before immersion, and m_1is the mass of the specimen after t days of acid exposure. This standardized approach allowed for a direct assessment of the impact of the acid attack on the material's physical stability.

3. Experimental results

3.1 Tensile performance

The uniaxial tensile performance of the Engineered Geopolymer Composite (EGC) and Engineered Cementitious Composite (ECC) specimens at room temperature is graphically detailed in Fig. 2. A key observation across all tested coupon specimens was that the ultimate tensile strength was consistently greater than the first-crack stress. This outcome confirms that all EGC and ECC mixtures successfully exhibited the desired strain-hardening behavior accompanied by a distribution of multiple micro-cracks. The addition of fly ash resulted in a noticeable reduction in the initial cracking strength. For example, the FA-EGC and FAS-EGC mixtures displayed first-crack strengths of 2.60 MPa and 2.38 MPa, respectively. This represents a reduction of 47.27% and 51.70% compared to the 100% slag-based EGC (S-EGC). This reduction is primarily attributed to the lower calcium content of fly ash, which yields a weaker geopolymer matrix compared to the slag-rich counterpart. Conversely, the inclusion of fly ash was highly effective at enhancing the tensile ductility. The strain capacity increased significantly to 2.64% for FA-EGC and peaked at 3.21% for FAS-EGC. The mechanism behind this improvement involves the fly ash reducing the frictional and chemical bonding at the Polyvinyl Alcohol (PVA) fiber/matrix interface. A weaker interface promotes stable fiber pull-out and the formation of a higher frequency of micro-cracks with reduced average crack widths (G. Humur and Çevik 2022a). This observed phenomenon—where the addition of fly ash leads to lower initial cracking stress and reduced fracture energy, but higher strain capacity is consistent with the established principles of strain-hardening cementitious composites. While increased fly ash concentrations in EGC mixtures generally improve tensile ductility, research indicates that exceeding an optimal FA content can eventually lead to a decline in strain capacity (Şahmaran et al. 2011), highlighting the need for careful mix proportioning.

The development of a calcium silicate hydrate and calcium-aluminum-silicate-hydrate gel from GGBFS hydration and polymerization was facilitated by the synergic adhesion between fly ash and slag in the EGC mix. An intriguing outcome was achieved by adding 50% slag to the mixture: it increased the mixture's maximum tensile stress, first-crack stress, and strain capacity as compared with FA-EGC specimens (Nath and Kumar 2013). Same findings were got in the authors' earlier study (G. Humur and Çevik 2022b), which showed that an increase in GGBFS quantity of up to 50% improved the strain capacity of EGC specimens.

However, when the percentage of GGBFS in the EGC mixes grew from 50% to 100%, strain capacity reduced by 26.69% and ultimate tensile strength increased by 89.62%. With an increase in GGBFS quantity, the ultimate tensile stress of EGC rose to 4.93 MPa for S-EGC (100% slag content) from 2.38 MPa for FA-EGC (zero slag content) and 2.60 MPa for FAS-EGC (50% slag content). Reason being, slag incorporation altered the geopolymer gels' chemistry, microstructurally compressed the EGC matrix, and produced a dense, low-porous material (Criado, Aperador, and Sobrados 2016). The tensile strength of the EGC combination with 100% fly ash binder was 4.7 MPa, as reported by Ling et al. (Ling et al. 2019). Similarly, EGC mixes with 10-30% GGBFS had tensile strengths between 5.7 and 6.8 MPa. The researchers also said that the EGC mixes, including slag, had better maximum tensile stress and first-crack strength than the EGC mixture containing 100% fly ash. However, these mixes had worse strain capacity, energy-performance index, and stress-performance index. While the EGC mix outperformed the S-EGC mix in terms of ultimate tensile strength (75.38%), it lagged behind the FAS-EGC mix by 7.5%. Lightweight EGCs nevertheless had a greater strain capacity than their ECC mix counterparts; FA-EGCs had a 6% increase and FAS-EGCs a 28.91% boost in strain capacity compared to the ECC mix. A higher tensile strength is achieved when a cement binder is added to an ECC matrix. The cement binder has a higher calcium content and speeds up the reaction rate of the ECC mixture.

The inclusion of fly ash in Engineered Geopolymer Composites (EGC) has a pronounced and well-documented effect on their mechanical response, particularly in the context of uniaxial tension, even when the Polyvinyl Alcohol (PVA) fiber volume fraction is held constant. Compared to slag-based mixtures, the presence of fly ash significantly enhances strain capacity (ductility) while simultaneously causing a reduction in fracture energy. This observed trade-off is fundamentally rooted in the modification of the matrix-fiber interfacial bond. Fly ash, typically being low in calcium (low-calcium Class F fly ash) and possessing relatively smooth particle surfaces, creates a weaker interfacial bond between the fiber and the geopolymer matrix (Kanda and Li 1998). A weaker interface is essential for promoting stable fiber pull-out rather than brittle fiber rupture, which, in turn, facilitates the formation of distributed micro-cracks across the specimen. The formation of numerous micro-cracks is the defining characteristic of strain-hardening behavior and leads directly to the observed increase in the composite's ultimate strain capacity. This mechanism aligns with the findings of Ling et al. (2025) (Ling, Y., Li, Z., Tan, Y., Yang, B. and Shi 2025), who highlighted that low-calcium matrices are critical for developing the weak fiber-matrix bond necessary for multiple cracking and high ductility in fiber-reinforced composites. The performance of fly ash-based EGCs is contrasted with the behavior of mixes rich in slag. Slag-rich geopolymer composites typically form a much denser matrix with stronger chemical bonding due to their higher calcium content. This strong bond often results in higher first crack and ultimate tensile strengths, but it sacrifices ductility. The strong interface limits the number of micro-cracks, leading to a localized crack pattern and a lower strain capacity, though the fracture energy is generally higher due to the greater work required to pull-out or rupture the strongly bonded fibers (Nematollahi et al. 2017; E.-H. Yang et al. 2009). Therefore, the findings in this study, where fly ash inclusion enhances deformability at the expense of energy absorption, are consistent with established literature in both ECC and EGC systems, which emphasizes that achieving desired tensile performance requires a careful balance between the matrix toughness and the fiber bridging capacity (Nematollahi, Sanjayan, and Ahmed Shaikh 2015).

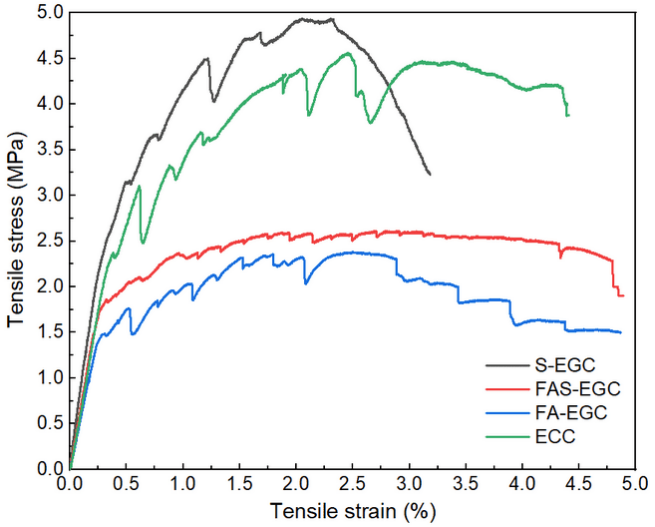

Fig. 2 Uniaxial tensile stress-strain curves of room temperature cured ECC and EGC specimens.

3.2 Visual appearance

The visual appearance of the Engineered Geopolymer Composite (EGC) and Engineered Cementitious Composite (ECC) specimens after exposure to the 5% H2SO4 solution for 60 and 120 days is presented in Fig. 3, alongside their unexposed control counterparts for direct comparison. Overall, the lightweight EGC specimens demonstrated superior resistance to the acid environment, exhibiting minimal to no discernible physical damage throughout the 120-day exposure period. The specimens containing slag as a binder (S-EGC and FAS-EGC) displayed a gradual surface color change from gray to a notable white hue. This coloration intensified as the slag content within the mixture increased and with prolonged exposure to the H2SO4 solution. Furthermore, a thin, crystalline layer of gypsum was observed forming on the surface, which became more pronounced over time. This finding aligns with microstructural studies suggesting that the reaction products responsible for the white coloration in high-slag mixtures are gypsum and ettringite (Qu et al. 2021). In contrast, the FA-EGC specimens, which utilized low-calcium fly ash, retained their uniform surface color and showed no significant visual degradation, even after 120 days of aggressive exposure. The lightweight ECC samples, which were initially light gray, showed pronounced visual deterioration upon 120-day exposure to the H2SO4 solution, primarily characterized by a distinct color shift from light gray to yellow. The accelerated damage observed in the ECC specimens compared to the EGCs is attributed to their higher calcium oxide (CaO) content, which increases the material's chemical reactivity when exposed to acidic media. The yellow discoloration in the lightweight ECC samples is primarily caused by the dehydration of ettringite, a common degradation product in Portland cement-based systems under acid attack (Sarkar and Mitra 2019; Speziale et al. 2008). Similar color transformations in ECC materials following acid exposure have been consistently reported in previous investigations (Gülcsan et al. 2019; Mehta and Siddique 2017).

Fig. 3 The visual aspect of EGC and ECC specimens after 60 and 120 days of exposure to a 5% H2SO4 solution

3.3 Dry density and Mass change

Figure 4 displays the densities of the EGC and ECC samples, which vary between 1700 and 1880 kg/m3. In comparison to the conventional ECC mix and the typical weight geopolymer concrete, this composition has a lower density. The primary reason for this is because recycled glass is utilized as a fine aggregate rather than silica sand. This is the key reason. Aside from S-EGC, all of the mix types studied fall into the category of structural lightweight concrete, which is defined as having a dry density below 1850 kg/m3 (Ries et al. 2010). Evidently, ECC and EGC composites may have their densities reduced by substituting recycled glass with silica sand. The density of the EGC and ECC specimens was greatly reduced as a result of the addition of fly ash, and this reduction was proportional to the rise in the concentration of fly ash. According to Table 1, the FA-EGC specimen had the lowest density of all the ECC and EGC specimens. This was the case for all of the specimens. In comparison to slag, fly ash has a lower specific gravity, which is the primary reason for this phenomenon among fly ash.

The mass variation of ECC and EGC samples exposed to a 5% H2SO4 solution over 0-, 60- and 120-day periods is shown in Figure 5. Results show that all samples lost mass after 120 days at room temperature (Fig. 5a). The mass loss was -3.36% for FA-EGC samples and -0.30% for S-EGC samples, in that order. Furthermore, substantial mass losses were seen in the EGC samples that weighed less than the ECC samples. The control (unexposed) samples may have lost weight since all of the EGC samples were oven-cured for one day at 70°C. Constant hydration responses over lengthy curing periods could explain why lightweight ECC samples lose

weight. Mass losses were less in geopolymer concrete samples that included 100% slag compared to those that contained 100% fly ash, according to Kurtoğlu et al. (Kurtoglu, A.E., Alzeebaree, R., Aljumaili, O., Nis, A., Gulsan, M.E., Humur, G. and Cevik, A 2018).

Nevertheless, every single lightweight EGC and ECC sample exhibited weight gain after 60 and 120 days of exposure to 5% sulfuric acid solutions. The samples with the largest mass gains were FA-EGC, whereas the ones with the smallest were ECC. After 60 days in the H2SO4 solution, the weight increases for FA-EGC, FAS-EGC, S-EGC, and ECC were 8.78%, 5.54%, 4.41%, and 3.09%, respectively. Nevertheless, as seen in Figure 6b, the exposed samples' weights began to decrease as the acid exposure times became longer. For instance, when the exposure time was increased from 60 to 120 days, the mass of the ECC samples decreased from 3.09% to 0.16% and that of the FAS-EGC samples from 5.54% to 2.73%. It is possible that the significant weight gain in samples containing fly ash is due to the fact that fly ash has a lower density and includes pores from unreacted FA particles. As a result, FA-EGC and FAS-EGC samples have greater permeability than S-EGC samples. In contrast, slag's lower Blaine fineness (418 m^2/kg) may explain why samples bound with slag show less weight growth; this, in turn, reduces solution absorption due to the slag's low porosity and high density.

Fig. 4 Dry densities of EGC and ECC specimens

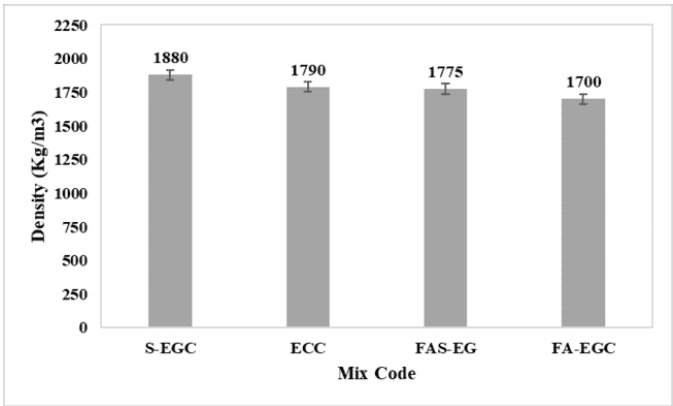

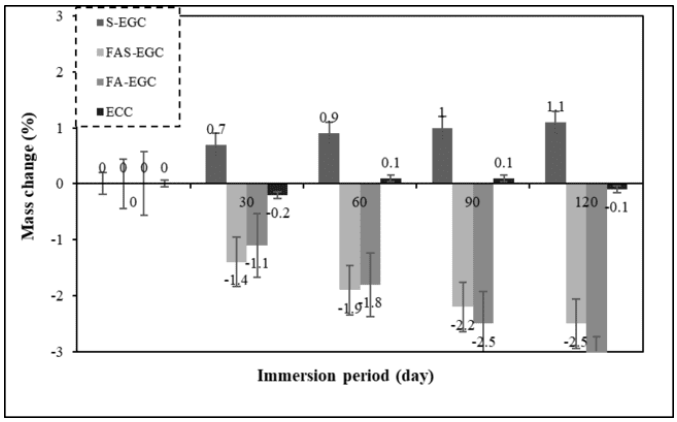

(a) Room temperature

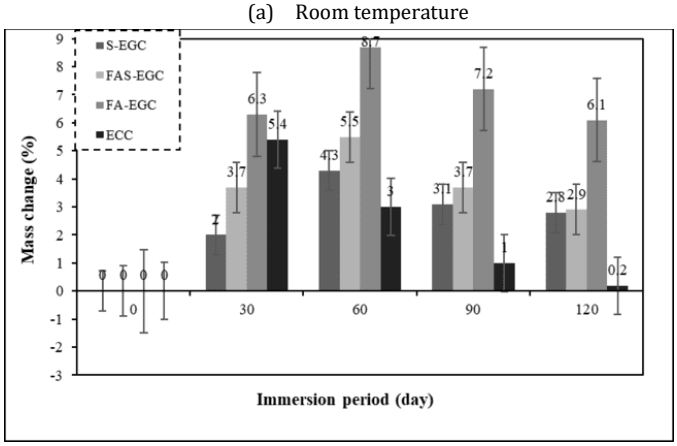

(b) 5% sulfuric acid

Fig. 5 Weight change of experimental specimens exposed to 5% H2SO4 solution up to 120 days

3.4 Compressive strength

Compressive strength tests were conducted on Engineered Geopolymer Composites (EGC) and Engineered Cementitious Composites (ECC) at 0-, 60- and 120-days following exposure to a 5% H_2SO_4 solution (Table 4, Figure 6). For unexposed specimens cured under ambient conditions for up to 120 days, compressive strengths ranged from 21.15 MPa to 63.7 MPa. Most ECC and EGC samples exceeded the minimum requirements for lightweight structural concrete (Prestera, Dixon, and Crocker 1990). Notably, specimens containing 100% slag (S-EGC) achieved the highest compressive strength, exceeding 60 MPa, comparable to high-strength concrete (ACI Committee 211 1998). Importantly, S-EGC represents a more sustainable alternative, as it eliminates the use of Portland cement, thereby reducing environmental impact. A significant increase in compressive strength was observed in EGC specimens with higher slag content. Compared to FA-EGC specimens, compressive strength increased by 166% at 50% slag content and by 301% at 100% slag content. This enhancement is attributed to the superior cementitious properties of ground granulated blast furnace slag (GGBFS), its higher CaO content, and its accelerated reaction kinetics relative to fly ash (FA). The elevated CaO concentration promotes early strength development and facilitates geopolymerization (Nath and Kumar 2013). Furthermore, the formation of calcium silicate hydrate (C-S-H) and calcium-aluminum-silicate hydrate (C-A-S-H) gels contribute to microstructural densification and improved mechanical performance (Nath and Kumar 2019). These hydration products reduce porosity and enhance the integrity of the EGC matrix (Fang et al. 2018). Conversely, the lowest compressive strengths were recorded for EGC samples containing fly ash, due to its lower reactivity and calcium content. The larger particle size of fly ash also contributes to reduced strength development (Chi and Huang 2013) Zhu et al. (Zhu, Yang, and Yao 2012) reported that ECC mixtures containing 70% fly ash and 0% slag exhibited the lowest compressive strength at 3, 14, 28, and 90 days, compared to mixtures with 40% fly ash and 30% slag. This discrepancy was partly due to a lower water-to-binder ratio in ECC. Compressive strength retention (%) of ECC and EGC samples exposed to a 5% H_2SO_4 solution at various ages is presented in Table 4 and Figure 7. All samples experienced strength degradation upon exposure, with more pronounced losses at longer durations. After 60 days, retained compressive strength for S-EGC, FA-EGC, FAS-EGC, and ECC specimens were 98%, 90.09%, 79.89%, and 71.75%, respectively. Among these, S-EGC exhibited the best mechanical performance and acid resistance. Both FA-EGC and FAS-EGC demonstrated superior durability compared to ECC.

Lightweight ECC and EGC samples showed increasing degradation with prolonged exposure to sulfuric acid. However, EGC samples, due to their lower calcium content, exhibited better acid resistance than ECC. The sodium aluminosilicate hydrate (N-A-S-H) gel formed in EGC was not subject to decalcification, unlike the calcium silicate hydrate (C-S-H) in ECC, contributing to a more stable structure under acidic conditions (N. K. Lee and Lee 2016). After 120 days of exposure, the retained strengths of S-EGC, FA-EGC, and FAS-EGC samples were 81.59%, 70.5%, and 68.05%, respectively. The superior durability of S-EGC is attributed to its dual reaction mechanism, producing both calcium silicate hydrate and calcium aluminosilicate hydrate gels. In contrast, FA-EGC relies primarily on N-A-S-H gel formation. Juenger et al. (Juenger et al. 2011) found that slag-based geopolymer concrete forms a well-crosslinked C-A-S-H gel with a high water-binding capacity, reducing permeability and enhancing durability, unlike FA-based geopolymers with lower water retention.

The compressive strength retention of the Engineered Geopolymer Composite (EGC) and Engineered Cementitious Composite (ECC) specimens after 120 days of exposure to 5% H2SO4 provided key insights into their acid resistance. Overall, the S-EGC (slag-based) mixture exhibited the superior durability and highest compressive strength retention, followed by FA-EGC and FAS-EGC. In contrast, the Portland cement-based ECC suffered the greatest strength loss at 42.57% after 120 days of exposure. The FAS-EGC samples displayed slightly lower residual strength (68.05%) compared to FA-EGC (70.50%). This finding is primarily attributed to the lower inherent acid resistance of the calcium-rich reaction products in the blended matrix, such as the sodium calcium aluminosilicate hydrate (N-C-A-S-H) gel, when contrasted with the pure sodium aluminosilicate hydrate (N-A-S-H) gel dominant in the 100% FA-EGC (N. K. Lee and Lee 2016). These results align with previous studies on geopolymer concrete durability: Mehta and Siddique (Mehta and Siddique 2017) reported a 33.18% strength loss for FA-based geopolymer concrete exposed to 2\% H2SO4. Alzeebaree et al. (Radhwan Alzeebaree et al. 2019) observed strength reductions of 30.3% and 40.6% in low-calcium FA-based geopolymer samples after 28 and 90 days, respectively, in a 5% sulfuric acid solution. Kurtoğlu et al. (Ahmet Emin Kurtoğlu, Radhwan Alzeebaree, Omar Aljumaili, Anıl Niş and Mehmet Eren Gülşan 2018) documented compressive strength losses of 17%, 32%, and 35% for slag-based geopolymer concrete after 30 days of H2SO4 exposure. The fundamental degradation mechanism in geopolymer composites under sulfuric acid exposure involves an initial ion exchange between the framework cations (e.g., Na+, K+) and the external sulfate ions. This is subsequently followed by the crystallization of gypsum within the deteriorated layer (Kani, Allahverdi, and Provis 2012; Vafaei et al. 2018). The higher acid resistance of slag-based EGC can be ascribed to the

formation of a denser, more chemically stable geopolymer matrix. This structural integrity limits the diffusion of aggressive ions and thus increases resistance to the structural breakdown induced by acid penetration and subsequent reaction product formation. The poor tensile strength observed in the oven-cured FAS-EGC is a consequence of several compounding factors related to the high-temperature curing regime: Microcracking from Internal Stresses: The rapid drying process at elevated temperatures induces significant internal stresses and microcracking within the matrix, which fundamentally compromises the material's integrity and ability to resist tensile forces (H. Zhang et al. 2014). Incomplete Polycondensation: Non-optimized high-temperature curing conditions can lead to incomplete polycondensation reactions, resulting in a weaker, less robust geopolymer network (Temuujin, van Riessen, and MacKenzie 2010). Brittle Matrix Formation: Oven-curing often yields a denser but more brittle matrix, reducing the composite's inherent ability to accommodate tensile deformation and strain-hardening (H. Zhang et al. 2014). Fiber-Matrix Bond Weakening: High curing temperatures can also degrade the crucial fiber-matrix interfacial bonding, limiting the effective stress transfer required for strain-hardening (W. K. W. Lee and Van Deventer 2002). Residual Thermal Stresses: Differences in the thermal expansion coefficients between the geopolymer matrix and the fly ash/slag particles create residual thermal stresses, further contributing to the degradation of the tensile properties (Hardjito and Rangan 2005). The combination of these effects explains the reduced tensile strength and ductility observed in the oven-cured FAS-EGC samples.

Table 4. Retained compressive power (%) of experimental specimens exposed to 5% H2SO4 solution

Exposure time (days)	FA-EGC	FAS-EGC	S-EGC	ECC
0	100	100	100	100
60	90.09	79.89	98	71.75
120	70.5	68.05	81.59	57.43

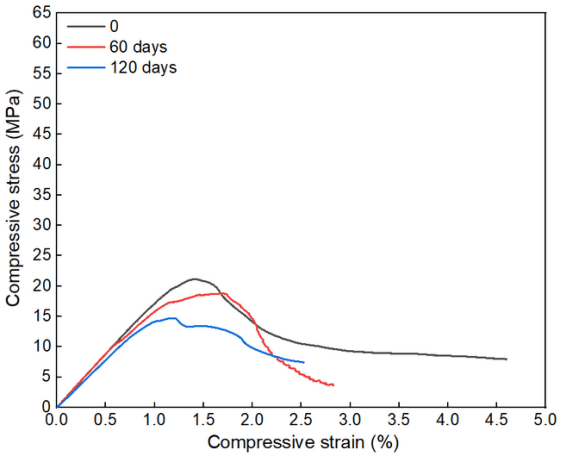

(a) FA-EGC

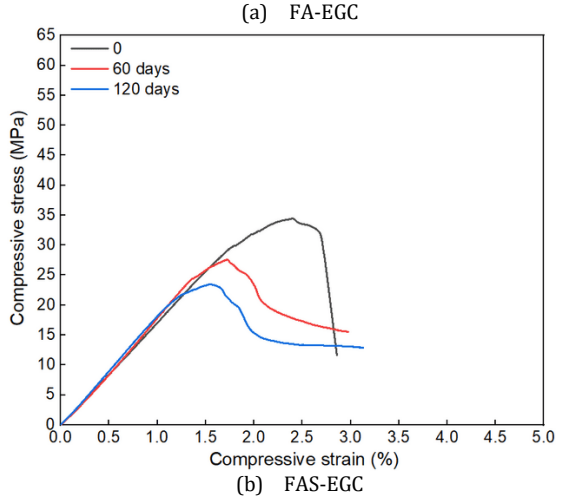

(b) FAS-EGC

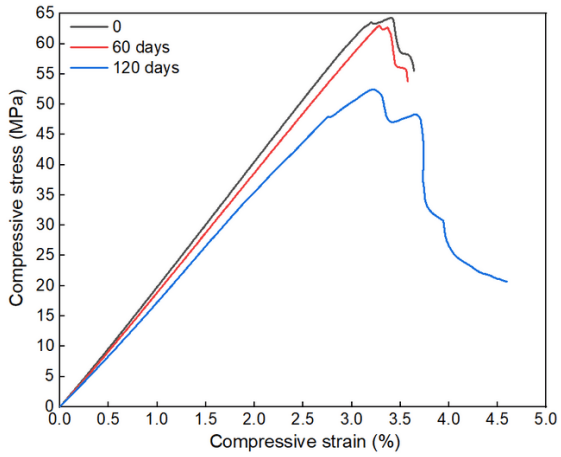

(c) S-EGC

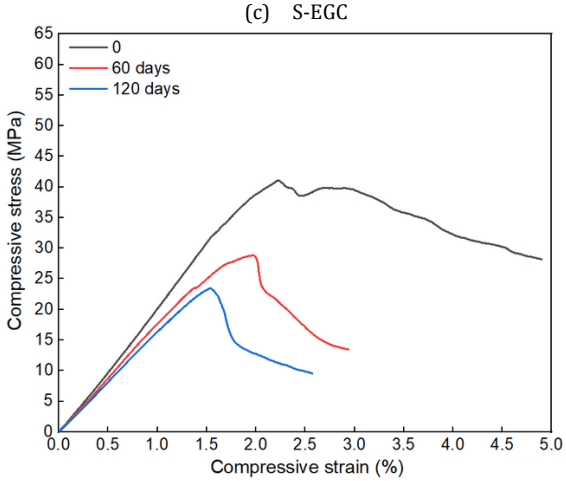

(d) ECC

Fig. 6 Compressive stress-strain responses of ECC and EGC specimens exposed to 5% H2SO4 solution for 0, 60, and 120 days

3.5 Flexural performance

Table 5 shows that as slag replacement levels grew, so did the maximum load. For example, compared to FA-EGC cured at normal temperature, the highest load of FAS-EGC and S-EGC at normal temperature (prior to sulfuric acid exposure) increased by 63.34% and 189.85%, respectively. The main reasons for these load increases were the improved matrix compactness of EGC and the matrix-fiber mixture after the addition of slag (Ling et al. 2019). However, for lightweight EGC with varying slag levels, the displacement property a measure of material ductility varied. In particular, displacement rose from 0 to 50% of the slag content but significantly reduced from 50% to 100% of the GGBFS content. For instance, FA-EGC, FAS-EGC, and S-EGC had displacements of 4.32 mm, 6.97 mm, and 2.52 mm, in that order. Therefore, up to 50% of slag added to the EGC matrix enhanced displacement. 50% fly ash and 50% slag-based EGC had the maximum deflection value. ECC deflection increased with increasing slag percentage from 10% to 30%, according to Zhu et al. (Zhu, Yang, and Yao 2012). Although the FA-EGC mix had a deflection that was 20.67% higher than the lightweight ECC mix, the maximum load increased by 122.5% due to the fly ash reaction rate relative to OPC.

The flexural performance of the lightweight Engineered Geopolymer Composite (EGC) and Engineered Cementitious Composite (ECC) samples, specifically their degradation in terms of maximum load and deflection capacity after 60 and 120 days of immersion in a 5% H2SO4 solution, is illustrated in Figure 7. Consistent with other mechanical tests, all samples exhibited maximum deterioration after the full 120-day exposure period. The impact of the acid attack on flexural properties was found to be analogous to its effect on compressive strength. The retained peak flexural loads after exposure were quantified as shown in Table 6:

Table 5. load and displacement of experimental specimens exposed to acid attack

Exposure time (days)	FA-EGC		FAS-EGC		S-EGC		ECC	
	Max. load (N)	Displacement (mm)	Max. load (N)	Displacement (mm)	Max. load (N)	Displacement (mm)	Max. load (N)	Displacement (mm)
0	1724	4.32	2816	6.97	4997	2.52	3836	3.58
60	1504	2.54	2152	4.43	4482	1.68	2437	1.83
120	1284	2.68	1814	3.54	3868	2.21	2022	1.46

Table 6. The retained peak flexural loads after exposure

Composite Type	Retained Peak Load After 60 Days (%)	Retained Peak Load After 120 Days (%)
S-EGC	89.69%	77.40%
FA-EGC	87.23%	74.48%
FAS-EGC	76.42%	64.41%
ECC	63.53%	52.71%

The results clearly indicate that all lightweight EGC samples demonstrated superior resistance to sulfuric acid attack compared to the lightweight ECC specimens. The S-EGC (slag-based) mixture maintained the highest residual load, confirming the trend observed in the compressive tests. The loss in flexural load capacity is directly attributed to the disintegration of the core aluminosilicate bonds within the geopolymer structure upon exposure to H2SO4. The polymerization products of geopolymers, characterized by their stable aluminosilicate linkages, are inherently more resistant to acid attack. This contrasts with the degradation mechanism of geopolymer products, which, as reported by Bakharev (Bakharev 2005), involves depolymerization and the formation of unstable reaction products like zeolites, leading to strength reduction. Deflection capacity is a critical parameter for evaluating the health of ECC and EGC materials in corrosive environments. Despite the observed reduction in deflection caused by the H2SO4 attack, all produced samples maintained the characteristic deflection-hardening and multiple-cracking behavior of these composites, as demonstrated in Figure 8. Remarkably, the lightweight EGC and ECC samples retained approximately 50% of their original deflection capacity even after 120 days of 5% H2SO4 exposure. This finding contrasts with some earlier studies, such as the work by Ohno and Li (Ohno and Li 2019), who reported that the displacement capacity of ECC could sometimes be enhanced after acid exposure. This enhancement was attributed to the degradation of the Ordinary Portland Cement (OPC) matrix, which reduced the matrix's tensile strength, thereby improving ductility and deflection-hardening behavior (Ohno and Li 2019). Similarly, Wang et al. (Tianyu Wang, Duo Zhang, He Zhu, Baosong Ma 2022) noted that after just seven days in a 1% H2SO4 solution, pulled-out fibers showed signs of significant surface abrasion and peeled-off fibrils. Given these complex and sometimes contrasting observations on fiber behavior and matrix degradation, further research is required to fully understand the long-term influence of Polyvinyl Alcohol (PVA) fibers and their interfacial bonding in highly aggressive chemical environments. The experimental data presented here serve as an important initial database on the behavior of tailored lightweight geopolymer composites when subjected to sulfuric acid attack.

The results of the present study were compared to the previous studies and summarized as shown in Table 7:

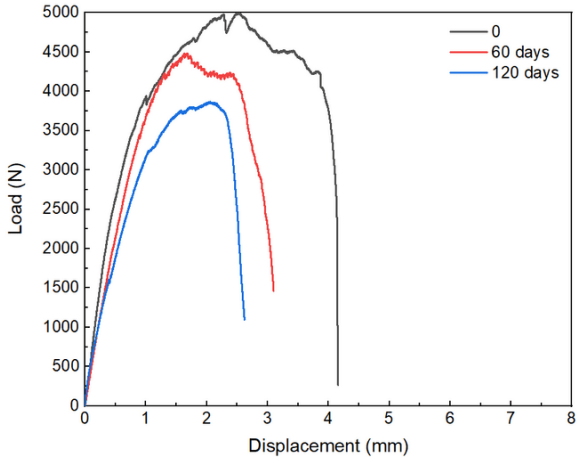

(a) S-EGC

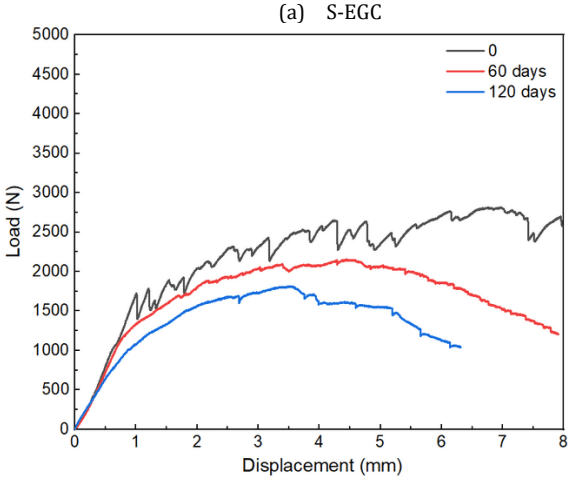

(b) FAS-EGC

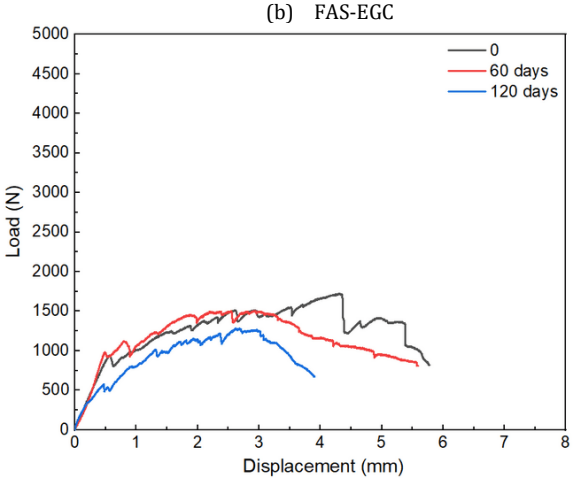

(c) FA-EGC

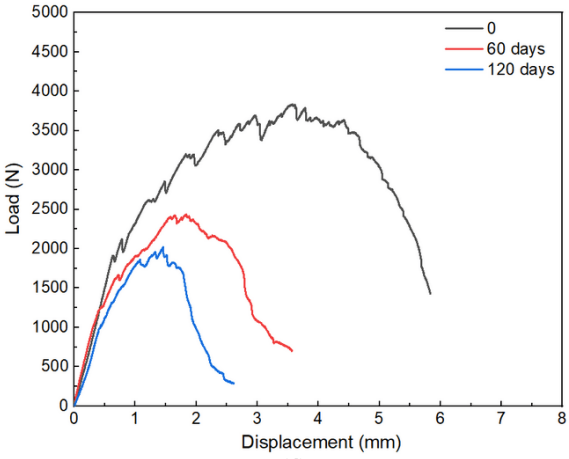

(d) ECC

Fig. 7 Load-displacement curves of experimental specimens exposed to 5% H2SO4 solution for 0, 60 and 120 days

Table 7. Summary of comparison between the present study and previous studies

Study	Type of Composite	Acid Type & Concentration	Exposure Duration	Retained Compressive Strength (%)	Retained Tensile Strength (%)	Key Observations
Ohno & Li (2019) [1]	ECC (Portland-based)	H_2SO_4, 5%	90 days	60–70	65	Matrix dissolution and fiber debonding were observed
Alzeebaree et al. (2019) [2]	EGC (Fly ash/slag blend)	H_2SO_4, 3%	120 days	75–80	—	Improved resistance with higher slag content
Zhang et al. (2020) [3]	GPC (Slag-rich)	H_2SO_4, 5%	90 days	80	—	C–A–S–H gel stability improved acid durability
El-Gamal et al. (2021) [4]	EGC (Fly ash + PVA fiber)	H_2SO_4, 5%	60 days	70	60	Fiber bridging reduced crack propagation
Present Study (2025)	Lightweight EGC (Slag & Fly ash) and ECC	H_2SO_4, 5%	120 days	85–90 (EGC), 70 (ECC)	80 (EGC), 65 (ECC)	Lightweight slag-based EGC showed superior acid resistance and retained strain-hardening capacity

3.6 Scanning electron microscopy

For SEM analysis, both exposed and unexposed EGC and ECC specimens were sectioned into dimensions of approximately 10 mm × 10 mm × 10 mm using a low-speed diamond saw to minimize mechanical damage during cutting. Specimens were taken specifically from the peripheral region (0–1 cm below the surface), where the effects of H_2SO_4 exposure are most pronounced. Following sectioning, samples were gently rinsed with isopropanol to remove any surface debris and then dried in a vacuum desiccator at room temperature for 24 hours to prevent additional chemical reactions or microstructural changes. Once dried, the specimens were mounted onto standard aluminum SEM stubs using carbon adhesive tape to ensure firm and conductive placement. A thin layer of gold (Au) was then applied to the sample surfaces via sputter coating (typically at 20 mA for 90 seconds) to enhance electrical conductivity and minimize charging during imaging. The SEM analysis focused on evaluating the microstructural changes in the EGC and ECC specimens before and after exposure to sulfuric acid (H_2SO_4). Special attention was given to the interfacial transition zone (ITZ) between the geopolymer or cementitious matrix and the PVA fibers, as this region is critical in determining composite performance. In addition, the microscale degradation of PVA fiber surfaces due to acid exposure was investigated. For each specimen, two high-resolution scanning electron micrographs were captured—one prior to and one following H_2SO_4 exposure—to assess surface-level deterioration, as the initial effects of acid attack typically manifest on the outer regions before progressing inward. The selected imaging zone remained consistently within the 0–1 cm surface depth to ensure a representative and comparative analysis of acid-induced damage.

Figure 8 illustrates the interaction between the EGC matrix and the embedded PVA fibers. In the case of the FA-EGC and FAS-EGC specimens, the fiber surfaces appeared relatively smooth and clean after exposure (Fig. 8b and 8c), which may indicate a weaker bond between the matrix and the fibers. This observation suggests that the presence of fly ash may hinder the formation of a strong fiber-matrix interface due to reduced geopolymerization activity. In contrast, the S-EGC specimens demonstrated a significantly higher degree of fiber-matrix cohesion, as evidenced by the abundant deposition of geopolymerization products on the PVA fiber surfaces (Fig. 8a). This well-developed interfacial bonding is likely to enhance mechanical performance by providing stronger resistance during fiber pullout. The presence of tightly adhered geopolymer products along the fiber surfaces may contribute to increased energy absorption and improved toughness in the S-EGC composite (Ling et al. 2019).

The microstructure of the EGC and ECC samples, both unexposed (Figure 8) and after 120 days of H2SO4 exposure (Figures 8 and 9), was examined using scanning electron microscopy (SEM), yielding critical information on the degradation mechanisms. Figure 8 illustrates the microstructural differences between the unexposed EGC mixtures: The addition of 100% slag resulted in a more compact and consistent matrix with reduced void formation. The complete inclusion of Ground Granulated Blast-furnace Slag (GGBFS) powder promoted microstructural densification, which is a primary reason for the enhanced mechanical performance observed in S-EGC specimens (G. Humur and Çevik 2022b). FA-EGC, FAS-EGC, and ECC: These samples exhibited greater matrix heterogeneity, notably the presence of several spherical, unreacted fly ash particles, which were absent in the S-EGC samples. The microstructure of EGC and ECC samples exposed to H2SO4 for 120 days (Figs. 8 and 9) showed significant changes, particularly at the ITZ: Ettringite Formation: A notable increase in the formation of ettringite and associated micro-cracking was observed, especially at the ITZ of the EGC samples (Figs. 9a, b, and c). The formation and growth of ettringite caused the EGC samples to expand during the exposure period, resulting in weight gain and a subsequent weakening of the matrix-fiber bond. Comparison of Ettringite Levels: The ECC samples exhibited a much higher quantity of ettringite compared to the EGC samples. This severe damage in lightweight ECC is directly correlated with its high CaO content, which readily interacts with damaging sulfate ions under H2SO4 attack (Alaa Mohammedameen; Abdulkadir Çevik; Mehmet Eren Gülşan 2018; Radhwan Alzeebaree et al. 2019). This finding confirms that lightweight ECC suffered more severe chemical damage than lightweight EGC. The condition of the Polyvinyl Alcohol (PVA) fibers after 120 days of acid exposure varied significantly across the mixtures: S-EGC (Figure 10a): PVA fibers remained straight and smooth, showing no discernible surface damage from the acid treatment.ECC, FAS-EGC, and FA-EGC (Figure 10d): These fibers displayed signs of curvature. Furthermore, the surface of the ECC specimens showed prominent abrasion and peeled-off fibrils on the pulled-out fibers. This is a clear indication of fiber degradation and/or weakening of the fiber-matrix interface due to the acid attack (Tianyu Wang, Duo Zhang, He Zhu, Baosong Ma 2022). The microstructural evidence supports the macroscopic findings, clearly demonstrating that the EGC samples were less susceptible to the H2SO4 attack than the ECC samples. The acid exposure led to the degradation of the ITZ through ettringite formation and visible surface damage to the PVA fibers, particularly in the ECC and fly ash-containing EGCs. This combined damage to the fiber surface and the ITZ is the underlying cause for the observed decrease in mechanical performance and the deflection-hardening behavior of the ECC and EGC specimens subjected to H2SO4.

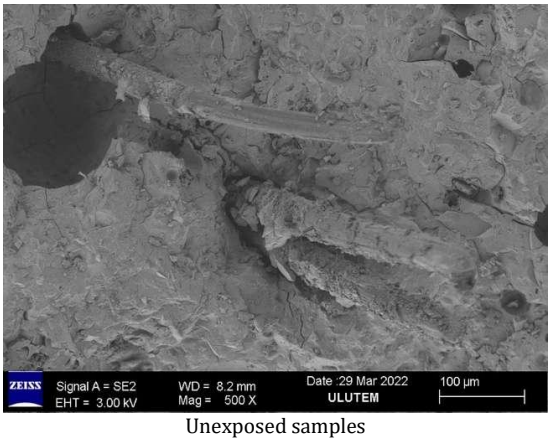

Unexposed samples

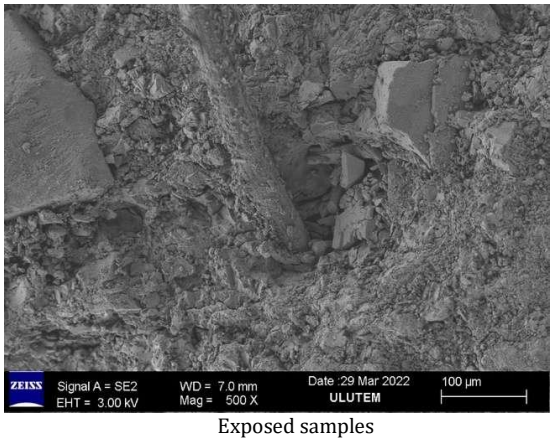

Exposed samples

(a) S-EGC

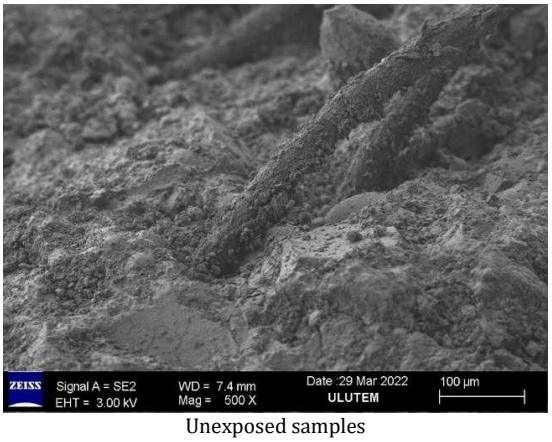

Unexposed samples

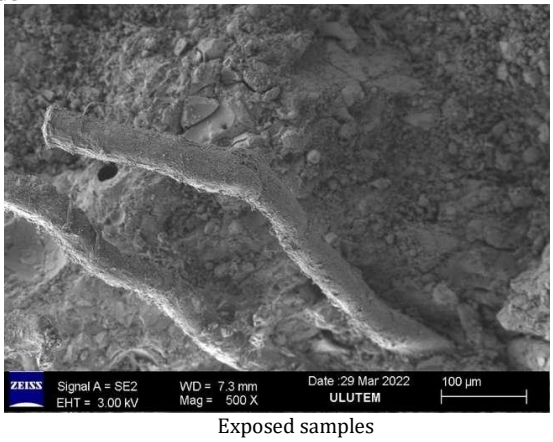

Exposed samples

(b) FAS-EGC

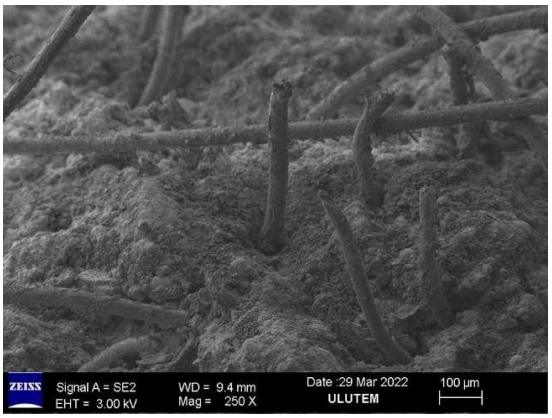

Unexposed samples

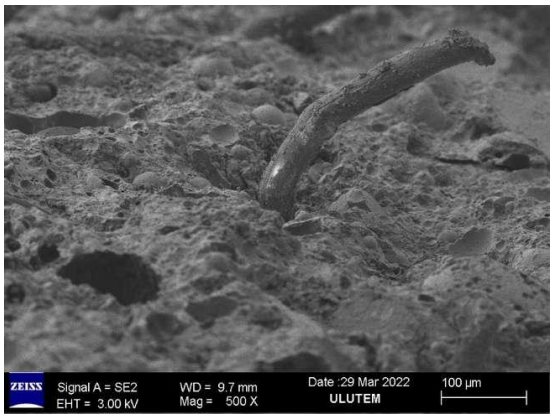

Exposed samples

(c) FA-EGC

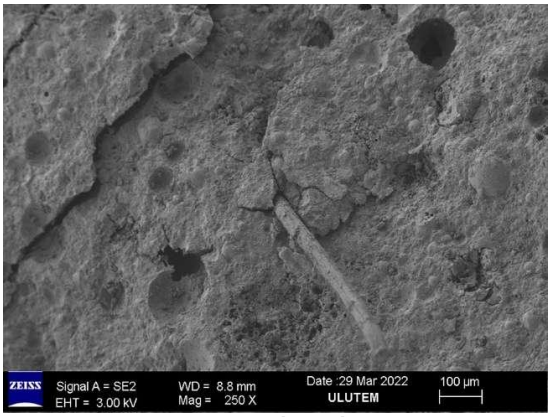

Unexposed samples

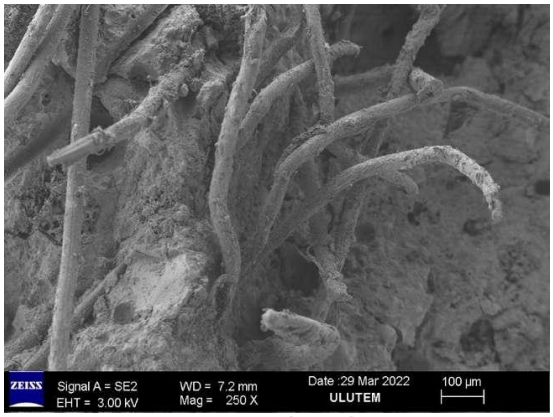

Exposed samples

(d) ECC

Fig. 8 SEM analysis of PVA fiber-reinforced EGC and ECC samples, both exposed and unexposed to a 5% H2SO4 solution

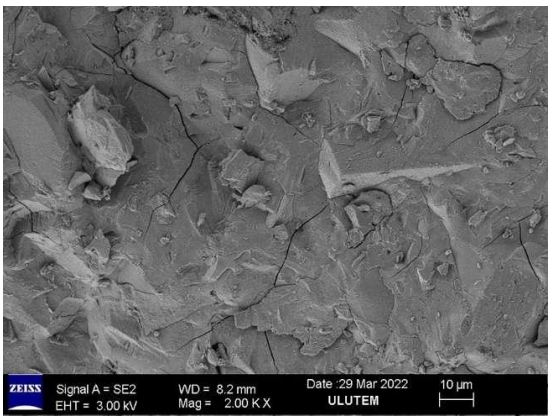

Unexposed samples

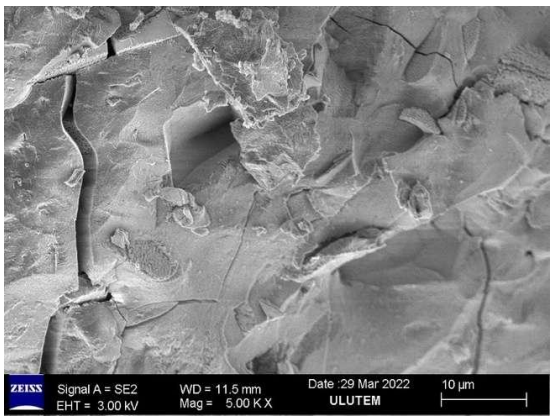

Exposed samples

(a) S-EGC

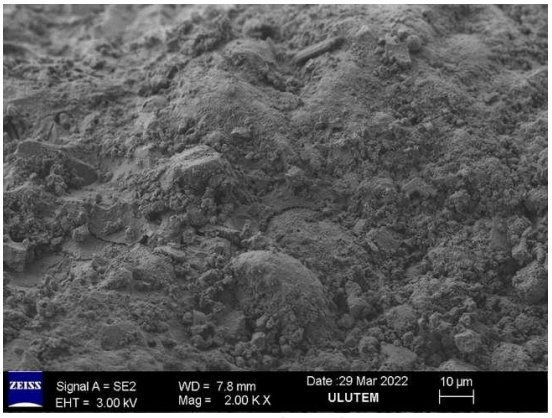

Unexposed samples

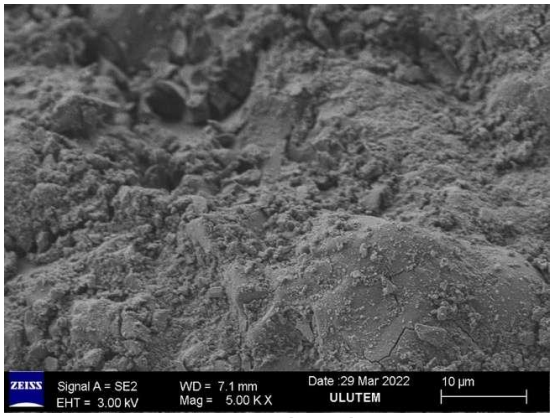

Exposed samples

(b) FAS-EGC

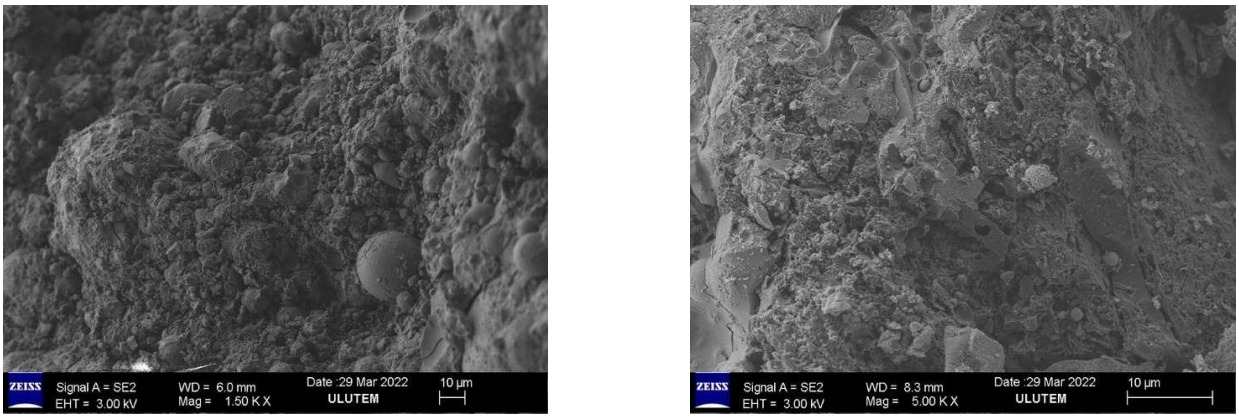

Unexposed samples

Exposed samples

(c) FA-EGC

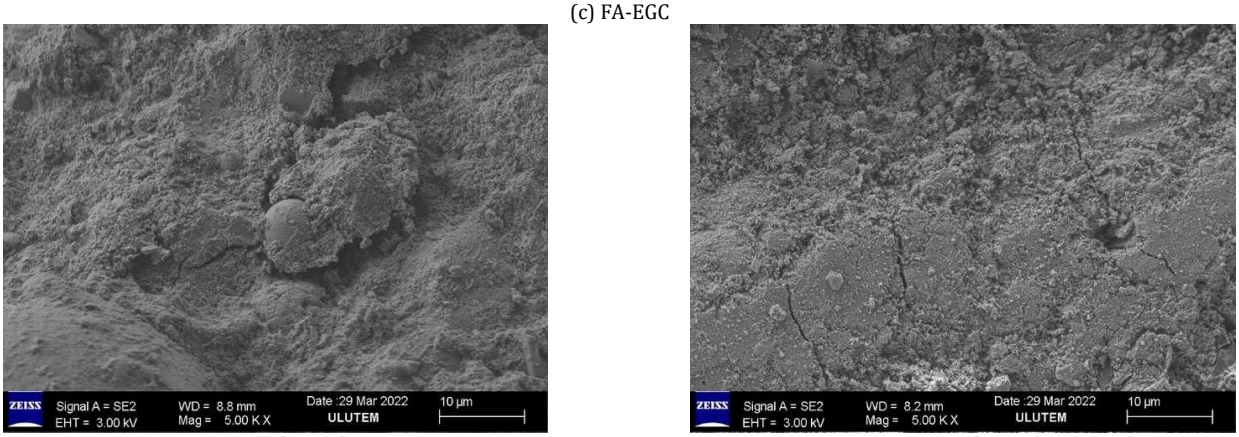

Unexposed samples

Exposed samples

(d) ECC

Fig. 9 SEM analysis of the matrix of EGC and ECC samples, both exposed and unexposed to a 5% H2SO4 solution

4. Conclusions

This study successfully investigated the mechanical properties and durability of lightweight Engineered Geopolymer Composites (EGCs) reinforced with Polyvinyl Alcohol (PVA) fibers, focusing on the influence of varying slag content. The performance of these composites after up to 120 days of exposure to a 5% H2SO4 solution was critically compared against that of lightweight Engineered Cementitious Composites (ECCs). The main conclusions drawn from the experimental results are summarized below:

1. All EGC and ECC specimens exhibited deflection-hardening and strain-hardening behavior under both flexural and uniaxial tensile loading.
2. Incorporating 50% slag (FAS-EGC) significantly improved first cracking stress, ultimate tensile strength, compressive strength, maximum flexural load, strain capacity, and deflection compared to 100% fly ash EGC (FA-EGC).
3. Increasing the slag content to 100% (S-EGC) yielded the highest ultimate flexural and tensile strengths but resulted in a lower strain capacity and deflection, indicating a shift toward increased strength and reduced ductility (more brittle) beyond the 50% slag replacement level.
4. All specimens experienced weight gain after 120 days in the 5% H2SO4 solution, an effect primarily driven by the formation and crystallization of degradation products like gypsum and ettringite.
5. The EGC mixtures containing slag (S-EGC, FAS-EGC) showed significantly lower weight changes compared to the 100% fly ash EGC (FA-EGC), indicating improved physical and chemical resistance in the acidic environment.
6. The loss in compressive strength due to sulfuric acid exposure ranged from 18.41% to 31.95% for the lightweight EGC specimens.
7. The ECC specimens showed a considerably greater strength loss of 42.57%. This confirmed that EGCs, particularly those with lower calcium content, exhibit superior durability against acid attack compared to their conventional ECC counterparts.
8. Both EGC and ECC specimens maintained a substantial level of deflection-hardening behavior and multiple cracking patterns even after prolonged acid exposure. Approximately 50% of the total deflection capacity was retained after 120 days in the aggressive sulfuric acid environment.
9. Microstructural analysis confirmed the greater resistance of lightweight EGCs over ECCs to sulfuric acid attack.
10. Among the EGCs, the 100% slag-based mix (S-EGC) showed the highest resistance, attributed to its denser, more chemically stable, cross-linked aluminosilicate polymer structure compared to the FA-EGC and FAS-EGC mixtures. Therefore, the incorporation of slag effectively enhances the chemical resistance of lightweight EGCs.
11. The overall enhanced mechanical and superior durability performance of the slag-containing EGC composites demonstrates their strong potential for use in aggressive environmental conditions, such as chemical processing plants, wastewater treatment facilities, and underground infrastructure exposed to acidic attacks.
12. The consistent retention of the strain-hardening and deflection capacity highlights the suitability of these lightweight EGCs for structural applications requiring both toughness and long-term durability against chemical degradation, positioning them as a sustainable alternative to conventional cementitious materials in harsh environments.

References

Abdulhaleem, Khamees N et al. 2025. "A Comprehensive Review of Sustainable Geopolymer Concrete Using Palm Oil Clinker: Environmental and Engineering Aspects." Energy Science & Engineering. https://doi.org/10.1002/ese3.1977

Abed, Mukhtar Hamid, Israa Sabbar Abbas, Majid Hamed, and Hanifi Canakci. 2022. "Rheological, Fresh, and Mechanical Properties of Mechanochemically Activated Geopolymer Grout: A Comparative Study with Conventionally Activated Geopolymer Grout." Construction and Building Materials 322: 126338. https://doi.org/10.1016/j.conbuildmat.2022.126338

ACI Committee 211. 1998. "ACI 211.4R-93 Guide for Selecting Proportions for High-Strength Concrete with Portland Cement and Fly Ash." Manual of Concrete Practice 93(Reapproved): 13.

ACI Committee 544, 2009. ACI 544.2R-89: Measurement of Properties of Fiber Reinforced Concrete (Reapproved 2009). American Concrete Institute, Farmington Hills, MI, USA.

Ahmet Emin Kurtoğlu, Radhwan Alzeebaree, Omar Aljumaili, Anıl Niş, and Ghassan Humur and Abdulkadir Çevik Mehmet Eren Gülşan. 2018. "Mechanical and Durability Properties of Fly Ash and Slag Based Geopolymer Concrete." Advances in Concrete Construction 6(4): 345-62.

Alaa Mohammedameen; Abdulkadir Çevik; Mehmet Eren Gülşan. 2018. "Mechanical Behavior and Durability of Confined and Unconfined Engineered Cementitious Composite Exposed to

Chemical Attack." Gaziantep University. https://doi.org/10.1016/j.conbuildmat.2019.02.108

Aljanabi, Maysam et al. 2022. "Residual Mechanical Performance of Lightweight Fiber-Reinforced Geopolymer Mortar Composites Incorporating Expanded Clay after Elevated Temperatures." Journal of Composite Materials 56(11): 1737-52. https://doi.org/10.1177/00219983221088902

Alzeebaree, R. et al. 2019. "Mechanical Properties and Durability of Unconfined and Confined Geopolymer Concrete with Fiber Reinforced Polymers Exposed to Sulfuric Acid." Construction and Building Materials 215. https://doi.org/10.1016/j.conbuildmat.2019.04.165

Alzeebaree, Radhwan et al. 2019. "Mechanical Properties and Durability of Unconfined and Confined Geopolymer Concrete with Fiber Reinforced Polymers Exposed to Sulfuric Acid." Construction and Building Materials 215: 1015-32. https://doi.org/10.1016/j.conbuildmat.2019.04.165

ASTM, 2019. ASTM C1609/C1609M-19: Standard Test Method for Flexural Performance of Fiber-Reinforced Concrete (Using Beam with Third-Point Loading). ASTM International, West Conshohocken, PA, USA.

Bakharev, T. 2005. "Resistance of Geopolymer Materials to Acid Attack." Cement and Concrete Research 35(4): 658-70. https://doi.org/10.1016/j.cemconres.2004.06.005

Chi, Maochieh, and Ran Huang. 2013. "Binding Mechanism and Properties of Alkali-Activated Fly Ash/Slag Mortars." Construction and Building Materials 40: 291-98. https://doi.org/10.1016/j.conbuildmat.2012.11.003

Criado, Maria, Willian Aperador, and Isabel Sobrados. 2016. "Microstructural and Mechanical Properties of Alkali Activated Colombian Raw Materials." Materials 9(3): 158. https://doi.org/10.3390/ma9030158

Fang, Guohao, Wing Kei Ho, Wenlin Tu, and Mingzhong Zhang. 2018. "Workability and Mechanical Properties of Alkali-Activated Fly Ash-Slag Concrete Cured at Ambient Temperature." Construction and Building Materials 172: 476-87. https://doi.org/10.1016/j.conbuildmat.2018.04.008

Gülcsan, Mehmet Eren et al. 2019. "Development of Fly Ash/Slag Based Self-Compacting Geopolymer Concrete Using Nano-Silica and Steel Fiber." Construction and Building Materials 211: 271-83. https://doi.org/10.1016/j.conbuildmat.2019.03.228

Gülşan, Mehmet Eren et al. 2018. "Effects of Sulphuric Acid on Mechanical and Durability Properties of ECC Confined by FRP Fabrics." Advances in Concrete Construction 2(6): 199-220.

Güneş, Muhammet, Hatice Öznur Öz, and Hasan Erhan Yücel. 2024. "The Properties of High-Ductility Engineered Geopolymer Composites Developed with Different Design Parameters." European Journal of Environmental and Civil Engineering: 1-25. https://doi.org/10.1080/19648189.2024.2445553

Hardjito, Djwantoro, and B Vijaya Rangan. 2005. "Development and Properties of Low-Calcium Fly Ash-Based Geopolymer Concrete." https://doi.org/10.1080/13287982.2005.11464946

Hardjito, Djwantoro, Steenie E Wallah, Dody M J Sumajouw, and B Vijaya Rangan. 2004. "On the Development of Fly Ash-Based Geopolymer Concrete." Materials Journal 101(6): 467-72. https://doi.org/10.1080/13287982.2005.11464946

Hu, Wei-Hsiu. 2023. "Decarbonization of Engineered Cementitious Composites (ECC)."

Humur, Ghassan, and Abdulkadir Çevik. 2022a. "Effects of Hybrid Fibers and Nanosilica on Mechanical and Durability Properties of Lightweight Engineered Geopolymer Composites Subjected to Cyclic Loading and Heating-Cooling Cycles." Construction and Building Materials 326(February): 1-33. https://doi.org/10.1016/j.conbuildmat.2022.126846

Humur, G. and Cevik, A., 2022b. "Mechanical Characterization of Lightweight Engineered Geopolymer Composites Exposed to Elevated Temperatures." Ceramics International. https://linkinghub.elsevier.com/retrieve/pii/S0272884222002607 (February 17, 2022).

Humur, Ghassan H et al. 2025. "Thermomechanical Properties of Slag-Based Engineered Geopolymer Composite under a Series of Cooling and Heating Cycles."

Humur, Ghassan Hussein, and Abdulkadir Çevik. 2024. "Magnesium Sulfate Resistance of Strain-Hardening Fiber Reinforced Slag and Fly Ash-Based Engineered Geopolymer Composites." Arabian Journal for Science and Engineering 49(4): 5909-25. https://doi.org/10.1007/s13369-023-08480-7

Japan Society of Civil Engineers. 2008. "Recommendations for Design and Construction of High-Performance Fiber Reinforced Cement Composites with Multiple Fine Cracks (HPFRCC)." Concrete Engineereing Series 82: Testing Method 6-10.

Juenger, M C G, F Winnefeld, J L Provis, and J H Ideker. 2011. "Cement and Concrete Research Advances in Alternative Cementitious Binders." Cement and Concrete Research 41(12): 1232-43. https://doi.org/10.1016/j.cemconres.2010.11.012

Kanda, Tetsushi, and Victor C Li. 1998. "Multiple Cracking Sequence and Saturation in Fiber Reinforced Cementitious Composites." https://doi.org/10.3151/crt1990.9.2_19

Kani, Ebrahim Najafi, Ali Allahverdi, and John L Provis. 2012. "Efflorescence Control in Geopolymer Binders Based on Natural Pozzolan." Cement and Concrete Composites 34(1): 25-33. https://doi.org/10.1016/j.cemconcomp.2011.07.007

Kurtoglu, A.E., Alzeebaree, R., Aljumaili, O., Nis, A., Gulsan, M.E., Humur, G. and Cevik, A. 2018. "Mechanical and Durability Properties of Fly Ash and Slag Based Geopolymer Concrete." Advances in Concrete Construction 6(4): 345-62.

Lao, Jian-Cong et al. 2023. "Strain-Hardening Alkali-Activated Fly Ash/Slag Composites with Ultra-High Compressive Strength and Ultra-High Tensile Ductility." Cement and Concrete Research 165: 107075. https://doi.org/10.1016/j.cemconres.2022.107075

Lao, J. C., Ma, R. Y., Xu, L. Y., Li, Y., Shen, Y. N., Yao, J., ... & Huang, B. T., 2024. "Fly Ash-Dominated High-Strength Engineered/Strain-Hardening Geopolymer Composites (HS-EGC/SHGC): Influence of Alkalinity and Environmental Assessment." Journal of Cleaner Production 447: 141182. https://doi.org/10.1016/j.jclepro.2024.141182

Lee, N. K., and H. K. Lee. 2016. "Influence of the Slag Content on the Chloride and Sulfuric Acid Resistances of Alkali-Activated Fly Ash/Slag Paste." Cement and Concrete Composites 72: 168-79. https://doi.org/10.1016/j.cemconcomp.2016.06.004

Lee, W K W, and J S J Van Deventer. 2002. "The Effect of Ionic Contaminants on the Early-Age Properties of Alkali-Activated Fly Ash-Based Cements." Cement and Concrete Research 32(4): 577-84. https://doi.org/10.1016/S0008-8846(01)00724-4

Li, Victor C. 2008. "Engineered Cementitious Composites (ECC) Material, Structural, and Durability Performance." In Concrete Construction Engineering Handbook, Chapter 24, Ed. E. Nawy, published by CRC Press. https://doi.org/10.1201/9781420007657.ch24

Li, V.C., 2019. Engineered Cementitious Composites (ECC): Bendable Concrete for Sustainable and Resilient Infrastructure. Springer.

Ling, Y., Li, Z., Tan, Y., Yang, B. and Shi, W. 2025. "Mechanical and Microscopic Performance of Engineered Cementitious Composites: Effects of Fly Ash Fineness and Calcium Content." Journal of Sustainable Cement-Based Materials: pp.1-19. https://doi.org/10.1080/21650373.2025.2569843

Ling, Yifeng et al. 2019. "Effect of Slag on the Mechanical Properties and Bond Strength of Fly Ash-Based Engineered Geopolymer Composites." Composites Part B: Engineering 164: 747-57. https://doi.org/10.1016/j.compositesb.2019.01.092

Malhotra, V. M. 1999. "Making Concrete 'Greener' With Fly Ash." Concrete Internationa 21: 61-66.

Mehta, Ankur, and Rafat Siddique. 2017. "Sulfuric Acid Resistance of Fly Ash Based Geopolymer Concrete." Construction and Building Materials 146: 136-43. https://doi.org/10.1016/j.conbuildmat.2017.04.077

Mustafa, Ş, Mohamed Lachemi, Khandaker M A Hossain, and Victor C Li. 2009. "Cement and Concrete Research Internal Curing of Engineered Cementitious Composites for Prevention of Early Age Autogenous Shrinkage Cracking." 39: 893-901. https://doi.org/10.1016/j.cemconres.2009.07.006

Nath, S. K., and Sanjay Kumar. 2013. "Influence of Iron Making Slags on Strength and Microstructure of Fly Ash Geopolymer." Construction and Building Materials 38: 924-30. https://doi.org/10.1016/j.conbuildmat.2012.09.070

Nath, S.K. and Kumar, S., 2019. "Influence of Granulated Silico-Manganese Slag on Compressive Strength and Microstructure of Ambient Cured Alkali-Activated Fly Ash Binder." Waste and Biomass Valorization 10(7): 2045-55. https://doi.org/10.1007/s12649-018-0213-1

Nematollahi, Behzad, Ravi Ranade, Jay Sanjayan, and Sayanthan Ramakrishnan. 2017. "Thermal and Mechanical Properties of Sustainable Lightweight Strain Hardening Geopolymer Composites." Archives of Civil and Mechanical Engineering 17(1): 55-64. https://doi.org/10.1016/j.acme.2016.08.002

Nematollahi, Behzad, Jay Sanjayan, and Faiz Uddin Ahmed Shaikh. 2015. "Tensile Strain Hardening Behavior of PVA Fiber-

Reinforced Engineered Geopolymer Composite." Journal of Materials in Civil Engineering 27(10): 04015001. https://doi.org/10.1061/(ASCE)MT.1943-5533.0001242

Nematollahi, Behzad, Jay Sanjayan, and Faiz Uddin Ahmed Shaikh. 2015. "Strain Hardening Behavior of Engineered Geopolymer Composites: Effects of the Activator Combination." Journal of the Australian Ceramic Society 51(1): 54-60.

Nematollahi, B., Sanjayan, J. and Shaikh, F.U.A., 2016. "Matrix Design of Strain Hardening Fiber Reinforced Engineered Geopolymer Composite." Composites Part B: Engineering 89: 253-65.
https://doi.org/10.1016/j.compositesb.2015.11.039

Niş, Anıl et al. 2024. "Microstructural and Durability Assessment of Various Concrete Types under Different Chemical Environments." Iranian Journal of Science and Technology, Transactions of Civil Engineering: 1-14. https://doi.org/10.1007/s40996-024-01437-2

Niş, Anıl, Necip Altay Eren, and Abdulkadir Çevik. 2023. "Effects of Recycled Tyre Rubber and Steel Fibre on the Impact Resistance of Slag-Based Self-Compacting Alkali-Activated Concrete." European Journal of Environmental and Civil Engineering 27(1): 519-37. https://doi.org/10.1080/19648189.2022.2052967

Ohno, Motohiro, and V.C. Li. 2019. "Sulfuric Acid Resistance of Strain Hardening Fiber Reinforced Geopolymer." Indian Concrete Journal (December): 47-53.

Ohno, Motohiro, and Victor C. Li. 2014. "A Feasibility Study of Strain Hardening Fiber Reinforced Fly Ash-Based Geopolymer Composites." Construction and Building Materials 57: 163-68. https://doi.org/10.1016/j.conbuildmat.2014.02.005

Ohno, M. and Li, V.C., 2018. "An Integrated Design Method of Engineered Geopolymer Composite." Cement and Concrete Composites 88: 73-85. https://doi.org/10.1016/j.cemconcomp.2018.02.001

Prestera, Jay R., Donald E. Dixon, and David A. Crocker. 1990. "Standard Practice for Selecting Proportions for Structural Lightweight Concrete (ACI 211.2)." ACI Materials Journal 87(6): 638-51. https://doi.org/10.14359/1919

Qader, Diyar N et al. 2025. "A Systematic Review of Metakaolin-Based Alkali-Activated and Geopolymer Concrete: A Step toward Green Concrete." Reviews on Advanced Materials Science 64(1): 20240076. https://doi.org/10.1515/rams-2024-0076

Qu, Fulin et al. 2021. "Performance Deterioration of Fly Ash/Slag-Based Geopolymer Composites Subjected to Coupled Cyclic Preloading and Sulfuric Acid Attack." Journal of Cleaner Production 321(September): 128942. https://doi.org/10.1016/j.jclepro.2021.128942

Revathy, J, K K Yaswanth, and P Gajalakshmi. 2023. "Flexural Performance of GGBS-Based EGC Layered Reinforced Cement Concrete and Geopolymer Concrete Beams: A Retrofit Perspective." Innovative Infrastructure Solutions 8(10): 263. https://doi.org/10.1007/s41062-023-01236-0

Ries, John P et al. 2010. "Guide for Structural Lightweight-Aggregate Concrete Reported by ACI Committee 213." : 1-38.

Sá Ribeiro, Marilene G. et al. 2021. "Acid Resistance of Metakaolin-Based, Bamboo Fiber Geopolymer Composites." Construction and Building Materials 302(June): 124194. https://doi.org/10.1016/j.conbuildmat.2021.124194

Sabapathy, Lavaniyah et al. 2020. "Acid and Sulphate Attacks on a Rubberized Engineered Cementitious Composite Containing Graphene Oxide." Materials 13(14). https://doi.org/10.3390/ma13143125

Şahmaran, Mustafa et al. 2011. "Effect of Fly Ash and PVA Fiber on Microstructural Damage and Residual Properties of Engineered Cementitious Composites Exposed to High Temperatures." Journal of Materials in Civil Engineering 23(12): 1735-45. https://doi.org/10.1061/(ASCE)MT.1943-5533.0000335

Sahmaran, Mustafa, Mo Li, and Victor C Li. 2007. "Transport Properties of Engineered Cementitious Composites under Chloride Exposure." Materials Journal 104(6): 604-11. https://doi.org/10.14359/18964

Sarkar, Prodip Kumar, and Nilanjan Mitra. 2019. "Cement and Concrete Research Molecular Level Deformation Mechanism of Ettringite." Cement and Concrete Research 124(July): 105836. https://doi.org/10.1016/j.cemconres.2019.105836

Shumuye, Eskinder Desta et al. 2023. "Review on the Durability of Eco-Friendly Engineering Cementitious Composite (ECC)." Case Studies in Construction Materials 19: e02324. https://doi.org/10.1016/j.cscm.2023.e02324

Speziale, Sergio et al. 2008. "Cement and Concrete Research Single-Crystal Elastic Constants of Natural Ettringite." 38: 885-89. https://doi.org/10.1016/j.cemconres.2008.02.004

Temuujin, Jadambaa, Arie van Riessen, and K J D MacKenzie. 2010. "Preparation and Characterisation of Fly Ash Based Geopolymer Mortars." Construction and Building Materials 24(10): 1906-10. https://doi.org/10.1016/j.conbuildmat.2010.04.012

Thampy, Reshmi, Rambabu Dadi, and Shashi Kant Sharma. 2024. "Alternative Binder Materials in ECC-a Review." Innovative Infrastructure Solutions 9(12): 452. https://doi.org/10.1007/s41062-024-01725-w

Tianyu Wang, Duo Zhang, He Zhu, Baosong Ma, Victor C. Li. 2022. "Durability and Self-Healing of Engineered Cementitious Composites Exposed to Simulated Sewage Environments." Cement and Concrete Composites: 104500. https://doi.org/10.1016/j.cemconcomp.2022.104500

Vafaei, Mostafa, Ali Allahverdi, Peng Dong, and Nabil Bassim. 2018. "Acid Attack on Geopolymer Cement Mortar Based on Waste-Glass Powder and Calcium Aluminate Cement at Mild Concentration." Construction and Building Materials 193: 363-72. https://doi.org/10.1016/j.conbuildmat.2018.10.203

Wu, Hao Liang, Duo Zhang, Yan Jun Du, and Victor C. Li. 2020. "Durability of Engineered Cementitious Composite Exposed to Acid Mine Drainage." Cement and Concrete Composites 108(January): 103550. https://doi.org/10.1016/j.cemconcomp.2020.103550

Yang, En-Hua, Mustafa Sahmaran, Yingzi Yang, and Victor C Li. 2009. "Rheological Control in Production of Engineered Cementitious Composites." Materials Journal 106(4): 357-66. https://doi.org/10.14359/56656

Yang, Qingguo et al. 2025. "Research on the Influence of Engineered Cementitious Composite's Water-Cement Ratio and Fiber Content on the Mechanical Performance of Foam Lightweight Soil." Buildings 15(9): 1479. https://doi.org/10.3390/buildings15091479

Zahid, Muhammad, Nasir Shafiq, Siti Nooriza A. Razak, and Rana Faisal Tufail. 2020. "Investigating the Effects of NaOH Molarity and the Geometry of PVA Fibers on the Post-Cracking and the Fracture Behavior of Engineered Geopolymer Composite." Construction and Building Materials 265: 120295. https://doi.org/10.1016/j.conbuildmat.2020.120295

Zhang, Hai-yan, Venkatesh Kodur, Liang Cao, and Shu-liang Qi. 2014. "Fiber Reinforced Geopolymers for Fire Resistance Applications." Procedia engineering 71: 153-58. https://doi.org/10.1016/j.proeng.2014.04.022

Zhang, Yunhan, and Ke Chen. 2023. "Digital Technologies for Enhancing Crane Safety in Construction: A Combined Quantitative and Qualitative Analysis." Journal of Civil Engineering and Management 29(7): 604-20. https://doi.org/10.3846/jcem.2023.19574

Zhang, Zhigang et al. 2023. "Mechanical and Self-Healing Properties of Calcium-Sulfoaluminate-Cement-Based Engineered Cementitious Composites (ECC)." Journal of Building Engineering 77: 107512. https://doi.org/10.1016/j.jobe.2023.107512

Zhang, Zhigang, Jin Cheng Liu, Xiaoqing Xu, and Liqun Yuan. 2020. "Effect of Sub-Elevated Temperature on Mechanical Properties of ECC with Different Fly Ash Contents." Construction and Building Materials 262: 120096. https://doi.org/10.1016/j.conbuildmat.2020.120096

Zhu, Yu, Yingzi Yang, and Yan Yao. 2012. "Use of Slag to Improve Mechanical Properties of Engineered Cementitious Composites (ECCs) with High Volumes of Fly Ash." Construction and Building Materials 36: 1076-81. https://doi.org/10.1016/j.conbuildmat.2012.04.031

Disclaimer